

A comparative study of the spectra recorded at RRCAT synchrotron BL-8 dispersive EXAFS beamline with other beamlines

ABHIJEET GAUR^{1,*}, B D SHRIVASTAVA¹, S N JHA²,
D BHATTACHARYYA² and A POSWAL²

¹School of Studies in Physics, Vikram University, Ujjain 452 001, India

²Applied Spectroscopy Division, Bhabha Atomic Research Centre, Mumbai 400 085, India

*Corresponding author. E-mail: abhijeetgaur9@gmail.com

MS received 13 February 2012; revised 3 July 2012; accepted 24 July 2012

Abstract. The aim of the present work is to make a comparative study of the EXAFS spectra recorded at the BL-8 dispersive EXAFS beamline at 2 GeV Indus-2 synchrotron source at RRCAT, Indore (India) with those recorded at other synchrotron EXAFS beamlines, viz., X-19A at NSLS, BNL (USA), EXAFS wiggler beamline 4-1 at the SSRL (USA) and beamline 11.1 at ELETTRA (Italy). For this purpose, EXAFS spectra at Cu K-edge in copper metal have been recorded at these four beamlines. Further, EXAFS spectra at Cu K-edge in a copper complex have also been recorded at BL-8 beamline and beamline 11.1 at ELETTRA (Italy). The obtained experimental $\mu(E)$ data have been background-subtracted and then normalized. The normalized data have been then converted to $\chi(k)$ data, which have been Fourier-transformed and then fitted with the theoretical model, thereby yielding different structural parameters. It has been shown that the results obtained from the EXAFS spectra recorded at the BL-8 beamline are comparable with those obtained from other synchrotron EXAFS beamlines and also with the crystallographic results reported by earlier workers. The reliability, usefulness and data quality of the BL-8 beamline have been discussed.

Keywords. Energy-dispersive extended X-ray absorption fine-structure spectroscopy; beamline BL-8; Cu metal; Cu complex.

PACS No. 78.70.Dm

1. Introduction

X-ray absorption spectroscopy (XAS) refers to the details of how X-rays are absorbed by an atom at energies near and above the core-level binding energies of that particular atom. XAS is the modulation of an atom's X-ray absorption probability due to the chemical and physical states of the atom. The XAS is typically divided into two regimes: X-ray absorption near-edge spectroscopy (XANES) and extended X-ray absorption fine-structure spectroscopy (EXAFS). The term X-ray absorption fine structure (XAFS) is

a broad term that comprises both these spectroscopies [1,2]. XAFS spectroscopy is a unique tool for studying, at the atomic and molecular scales, the local structure around selected elements that are contained within a material. It can be applied not only to crystals, but also to materials that possess little or no long-range translational order: amorphous systems, glasses, quasicrystals, disordered films, membranes, solutions, liquids, metalloproteins – even molecular gases. This versatility allows it to be used in a wide variety of disciplines: physics, chemistry, biology, biophysics, medicine, engineering, environmental science, materials science and geology [3].

XAFS spectroscopy has developed hand in hand with the growth of synchrotron radiation research. Generally, two different types of beamline set-ups are commonly employed for recording XAFS spectra using synchrotron radiation. In the first type, a double crystal monochromator (DCM) is used and the XAFS measurements can be done in transmission, fluorescence and electron yield modes. In the second type, a bent crystal polychromator is used and the transmitted beam intensity from the sample is recorded on a position-sensitive CCD detector, thus enabling recording of the whole XAFS spectrum around an absorption edge in a single shot. This second type of EXAFS beamline set-up, named BL-8 dispersive EXAFS beamline, has been recently developed at the Indus-2 synchrotron source at the Raja Ramanna Centre for Advanced Technology (RRCAT), Indore [4–6]. In an earlier communication [7], we have described the various aspects of the calibration of the beamline, the procedure which should be followed for EXAFS measurements and the method to check the performance of the beamline. We have also reported the EXAFS study of hydroxo-bridged copper complexes using this beamline [8].

In the present work, we have done comparative study of the XAFS spectra recorded at the BL-8 beamline with those recorded at three other well-known synchrotron EXAFS beamlines, in order to evaluate the quality and reliability of the recorded data and the usefulness of the BL-8 beamline. For this purpose, XAFS spectra at Cu K-edge in copper metal have been recorded at (1) BL-8 dispersive EXAFS beamline at 2 GeV Indus-2 synchrotron source at RRCAT, Indore, India, (2) EXAFS beamline 11.1 at ELETTRA Synchrotron Light Laboratory, Basovizza, Italy, (3) EXAFS beamline X-19A at National Synchrotron Light Source (NSLS), Brookhaven National Laboratory, Upton, New York, USA and (4) EXAFS wiggler beamline 4-1 at the Stanford Synchrotron Radiation Laboratory (SSRL), Stanford, California, USA. Also, the XAFS spectra at Cu K-edge in a copper complex (N,N'-ethylenebis(salicylideneiminato) copper(II)) have been recorded at the BL-8 beamline and beamline 11.1 at ELETTRA. The data have been processed and analysed using EXAFS data analysis programs *Athena* and *Artemis*. The background-subtracted and normalized experimental data have been Fourier-transformed and then fitted with the theoretical model, thereby yielding different structural parameters. The structural parameters obtained by using BL-8 beamline for copper metal and the copper complex have been compared to those obtained from other beamlines. The obtained bond lengths have been compared with the crystallographic results reported by earlier workers.

2. Experimental methods

The details of the four EXAFS beamlines, at the different synchrotron facilities, used in the present work are described below in brief. XAFS spectra at Cu K-edge in copper

metal have been recorded at these beamlines. Also, XAFS spectra at Cu K-edge in a copper complex (N,N'-ethylenebis(salicylideneiminato) copper(II)) have been recorded at the BL-8 beamline and beamline 11.1 at ELETTRA. All the measurements were made at room temperature.

Cu metal was in the form of foil. Foils varying in thickness from 5 to 8 μm have been used. Though the same foil was not used at different beamlines, the foils used were those available at different beamlines. It was however ascertained that the foils used were obtained from the same firm (Goodfellow Cambridge Ltd., Huntingdon, England).

The copper complex was finely powdered and then absorption screens were prepared by carefully spreading calculated amount of the powder on 1 cm^2 area of kapton tape. The samples were prepared such that the absorption was $\mu x = 1$ for copper and the total absorption for the sample was less than 2.7 [9]. For the complex, same absorption screens were used at both the beamlines and the measurements were made within a period of one month. As the complex used were quite stable and the samples were well-preserved in a desiccator, no change in the sample could have occurred within this period.

Beamline BL-8 at RRCAT, India: The dispersive EXAFS beamline BL-8 at Indus-2 synchrotron source at RRCAT has a beam energy of ~ 2 GeV and is described by Das *et al* and Bhattacharyya *et al* [4–6]. The beamline has a 460-mm long Si(1 1 1) crystal having $2d$ value equal to 6.2709 Å mounted on an elliptical bender, which can bend the crystal to take shape of an ellipse. The radiation transmitted through the sample was detected by a position-sensitive CCD detector. A plane mirror was then used before the detector to cut off the higher harmonics from the radiation diffracted by the Si crystal. The plot of absorption vs. photon energy was obtained by recording the intensities I_0 and I_t , as the CCD outputs, without and with the sample, respectively and using the relation, $I_t = I_0 e^{-\mu x}$, where μ is the absorption coefficient and x is the thickness of the absorber. Calibration was done using the method outlined by Gaur *et al* [7] in an earlier study. It is worth mentioning here that for the setting of the bent crystal to record the XAFS spectra at the K-edge of copper, the spectra can be recorded only up to ~ 300 eV (i.e., $k = 9 \text{ \AA}^{-1}$) above the edge.

The beamline has a resolution of 1 eV at 10 keV photon energy, same as that of the other three beamlines. However, the observed spectra (figures 1a and b) show a lesser resolution for BL-8 beamline. This may be due to the polychromator and the CCD detector used on this beamline. No correction has, however, been made for the difference observed in the resolution in different beamlines.

At this beamline, the incident intensity obtained at 2.0 GeV beam energy and 50–60 mA beam current was such that the CCD detectors gets saturated within a few microseconds when I_0 was measured. Hence, the typical time to record a spectrum could be only a few microseconds. If the time was increased, the detectors got saturated. Hence, we have taken a large number of spectra keeping the time a few microseconds and then summed them up. This increased the signal-to-noise ratio and good spectrum was obtained. This was why the noise in the data was low, though the beam current was 50–60 mA as compared to other beamlines having beam currents from 130 to 280 mA. Hence, it is advised that while using this beamline, a large number of spectra should be recorded for a sample and then data should be summed up.

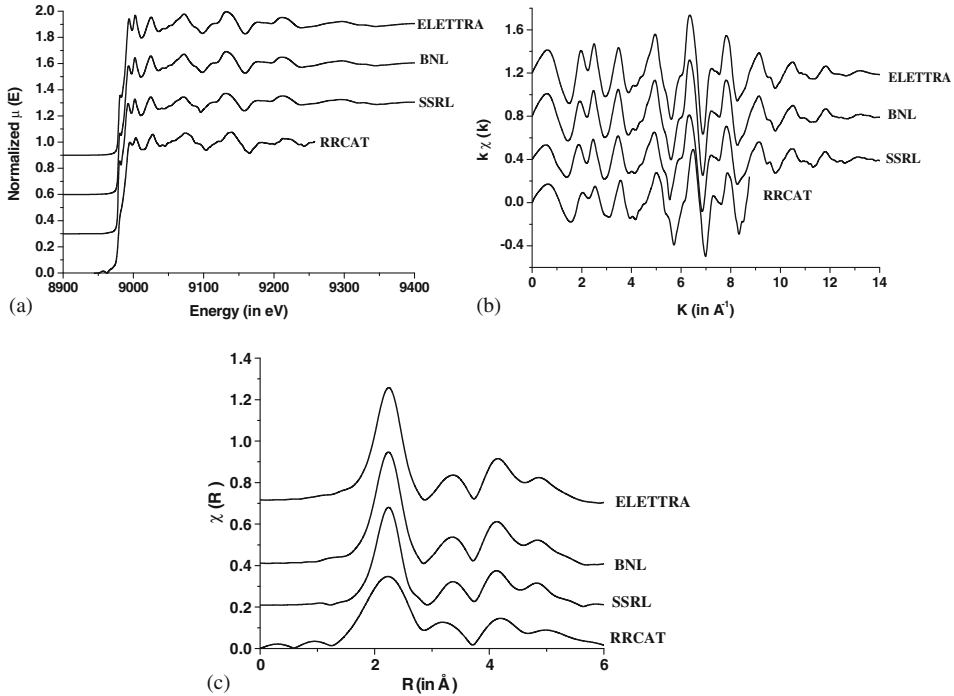


Figure 1. (a) Normalized Cu K-edge EXAFS spectra for metal obtained from four different synchrotron EXAFS beamlines. (b) k^1 -weighted $\chi(k)$ spectra obtained from normalized $\mu(E)$ spectra given in (a). (c) Fourier transform of the $\chi(k)$ spectra given in (b).

Out of the four beamlines used in the present work, three beamlines were DCM-based beamlines and on these beamlines, the beam was monochromatic at the sample and I_0 and I_t could be measured simultaneously. This is not possible at the BL-8 dispersive beamline for the obvious reason that the beam is polychromatic. This is a demerit of dispersive geometry. Therefore, we have measured I_0 just before and just after the transmission measurement and taken a mean of the two. In this procedure, it is assumed that the photon flux is not changing with time. This may not be always true and one may lose EXAFS signal at higher k values, where EXAFS signal is around 1% only.

Beamline X-19A at BNL, USA: The EXAFS beamline X-19A at National Synchrotron Light Source (NSLS), Brookhaven National Laboratory, Upton, New York, USA has 2.8 GeV beam energy and 280 mA current. A double silicon crystal Si(1 1 1) was used as the monochromator. Harmonics were suppressed by detuning the crystal spectrometer. The XAFS data at the K-absorption edge of copper were obtained in the transmission mode at room temperature. Three ionization chambers were employed as detectors. For each spectrum, the integration time was 0.5 s, the delay time was 0.3 s and the total numbers of points recorded were 510. At least three runs were taken for each sample. Energy was calibrated by setting the first inflection point of the copper metal K absorption edge to 8979 eV [10].

Beamline 11.1 at ELETTRA, Italy: The EXAFS beamline 11.1 at the ELETTRA Synchrotron Light Laboratory, Basovizza, Italy has the storage ring operated at 2.37 GeV with a typical current of 130 mA [11,12]. An internal reference of copper foil was used for energy calibration at each scan. Data were acquired in transmission mode. The white beam was monochromatized using a fixed exit monochromator equipped with a pair of Si(1 1 1) crystals. Harmonics were rejected by using the cut off of the reflectivity of the platinum mirror placed at 3 mrad with respect to the beam upstream the monochromator and by detuning the second crystal of the monochromator by 30% of the maximum. XAFS spectra were collected from 8830 eV to 10000 eV in the constant k mode. Integration time from 8940–9010 being 0.5 s, maximum integration time was 5 s. The energy was defined by assigning the first inflection point of the Cu foil spectrum to 8979 eV.

Beamline 4-1 at SSRL, USA: The EXAFS wiggler beamline 4-1 at the Stanford Synchrotron Radiation Laboratory (SSRL), Stanford, California, USA has a double silicon crystal Si(1 1 1), which is used as monochromator. It has energy range of 5,500–38,000 eV with an energy resolution of 10^{-4} . The spot size of the beam obtained is 4×18 mm. Harmonics were suppressed by detuning the crystal spectrometer. The XAFS data at the K-absorption edge of copper were obtained in the transmission mode. Three ionization chambers were employed as detectors. The energy of the first inflection point of the copper metal K absorption edge was taken as 8979 eV for this purpose. (Details can be found at www.ssl.slac.stanford.edu/beamlines/bl4-1.)

In the following sections, the XAFS data recorded at these four beamlines have been abbreviated as RRCAT data, BNL data, ELETTRA data and SSRL data, respectively.

3. Data analysis

The data have been analysed using the available computer software packages *Athena* version 0.8.056 and *Artemis* version 0.8.012 [13,14]) (available from www.xafs.org). These programs include AUTOBK [15] for background removal, FEFF6L [16] for generation of the theoretical EXAFS models, and FEFFIT [14] for parameter optimization of the model. A brief description of the procedure used for the analysis of the spectra is given below.

For normalizing the spectra, a linear function is regressed to the pre-edge region, and a linear or quadratic function is regressed to the post-edge region. Normalized $\mu(E)$ spectra are produced by subtracting the pre-edge line from the entire data spectrum and then dividing the spectrum by the step height. $\mu(E)$ data are then converted to $\chi(k)$ data. The $\chi(k)$ data are then Fourier-transformed in *Artemis*. To extract the information about the various parameters that can be determined from EXAFS data, the data have to be compared with a theoretical model using the standard EXAFS equation [17]. In the present work, we have generated the theoretical model by using *Artemis*. *Artemis* has a special interface called 'Atoms' that converts crystal structure information into a cluster of atoms and provides a list of atom positions in x , y , z coordinates for use in FEFF computations. This trial structure is given as input to the FEFF code to generate a theoretical EXAFS model. There are several adjustable parameters optimized by the computer code FEFFIT to fit the data. These parameters include the passive electron reduction factor (S_0^2),

Table 1. The input positional parameters for copper complex (from Bhadbhade *et al.* 1993).

Sl. No.	Element	x	y	z
1	Cu 1	0.23284	0.20565	0.09795
2	O1	0.28454	0.37650	0.06240
3	O2	0.18423	0.40820	0.08890
4	N1	0.28275	0.00200	0.12740
5	N2	0.18799	0.03110	0.15360
6	C1	0.33340	0.36370	0.09040
7	C2	0.36430	0.52150	0.07810

the number of identical paths (N_i), the relative mean-square displacement of the atoms included in path (σ_i^2), an energy shift for each path (ΔE_0), and a change in the path length (ΔR_i) [9].

In the present work, we have used the following parameters as inputs in *Artemis* for calculating the theoretical models.

Copper metal: Space group: fcc, Cell edge $a = 3.61 \text{ \AA}$, Core atom: Cu,
 $x = 0.0$, $y = 0.0$, $z = 0.0$, Cluster size = 7.0 \AA .
 Copper complex: Space group: C2/c, Cell constants:
 $a = 26.6580 \text{ \AA}$, $b = 6.9380 \text{ \AA}$, $c = 14.7190 \text{ \AA}$, and $\beta = 97.42^\circ$.
 Cluster size = 8 \AA .

The remaining input positional parameters for the complex are given in table 1 [18].

The theoretical models are adjusted as needed until the best possible fit is obtained between theoretical and experimental spectra, thereby the required parameters are obtained. The results obtained in the present study are discussed below.

4. Results and discussions

4.1 Copper metal

Figure 1a shows the normalized $\mu(E)$ vs. E spectrum at the K-absorption edge of copper metal obtained using the four different synchrotron EXAFS beamlines. Figure 1b shows their respective $\chi(k)$ vs. k plots and figure 1c shows their corresponding Fourier-transformed spectra. In these figures, the spectra have been shifted vertically by suitable values so that the spectra may be easily compared with each other. For the present analysis the input parameter R_{bkg} , that determines the maximum frequency of the background, was set to 1.20 \AA . The magnitude of the Fourier-transformed data $|\chi(R)|$ with k weighting of 1 are shown in figures 2a–d. In the case of RRCAT data, the Fourier transform was performed over the k -range: $k_{\text{min}} = 2.73 \text{ \AA}^{-1}$, $k_{\text{max}} = 8.52 \text{ \AA}^{-1}$, as it has already been pointed out that in the case of RRCAT data, the spectra could be recorded only up to $\sim 300 \text{ eV}$ (i.e., $k = 9 \text{ \AA}^{-1}$) above the edge. In order to keep the fitting on equal footing and

Comparative study of EXAFS beamlines

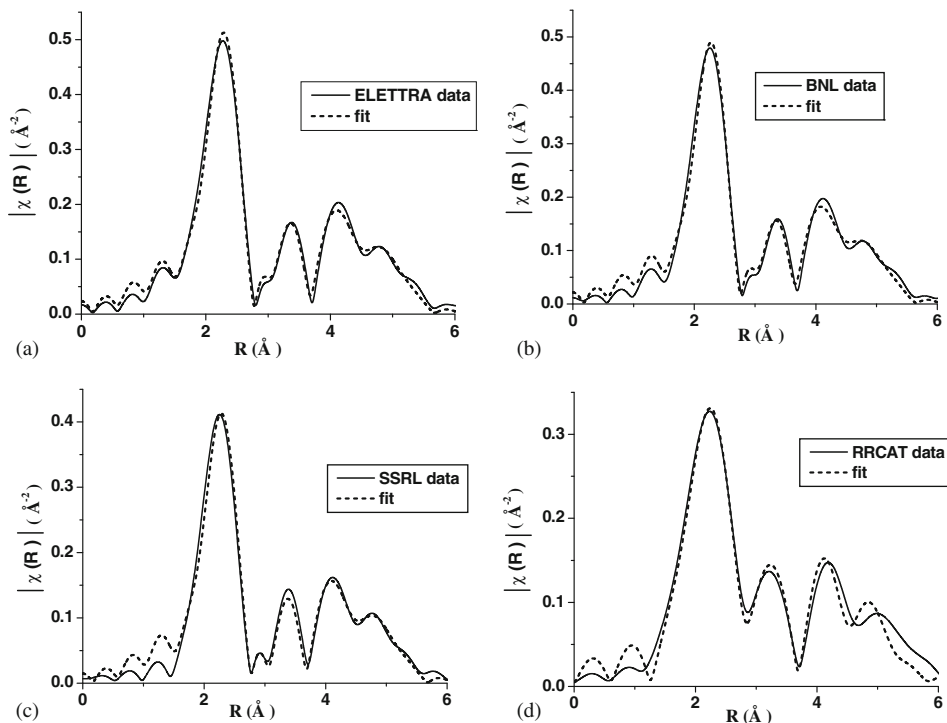


Figure 2. Magnitude of the Fourier transform of experimental data (solid line) along with theoretically modelled fit (dashed line). (a) ELETTRA, (b) BNL, (c) SSRL and (d) RRCAT data. The data have been fitted using k weight of 1. The fitting parameters are given in the text.

for better comparison of the results, the k range was kept the same for the data obtained from the other three beamlines, though their data were recorded up to $\sim 14 \text{ \AA}^{-1}$.

Theoretically modelled data were fitted in the R -space to the experimental data using $k_w = 1$ in each case. The fittings were performed for the first four coordination shells in all the four cases in the same R range of 1–5.5 \AA . This was done to present these data sources on equal footing for better comparison. In the fitting procedures, same selected paths were used in each case and the fits are also shown in figures 2a–d.

The results obtained from fitting are given in table 2, which gives the local structure parameters obtained from the EXAFS analysis for Cu metal. The S_0^2 values obtained are 0.86 ± 0.05 , 0.78 ± 0.06 , 0.70 ± 0.05 and 0.72 ± 0.14 for ELETTRA, BNL, SSRL and RRCAT data, respectively, and are comparable to each other. The different values of S_0^2 obtained from the different beamlines can be explained considering the fact that S_0^2 often differs for the same material due to beamline and sample attributes [19]. S_0^2 values lie within a general range of 0.7–1.1 and are affected by the differences in beamline parameters such as energy resolution, harmonic rejection, detector efficiency and differences in sample homogeneity and thickness.

The ΔE_0 values 5.49 ± 0.37 , 4.78 ± 0.44 , 4.94 ± 0.59 and 5.93 ± 0.89 for ELETTRA, BNL, SSRL and RRCAT data, respectively, are also comparable to each other. The values

Table 2. EXAFS fitting results for copper metal (at $T = 298$ K).

Beamlines at	1st shell			2nd shell			3rd shell			4th shell		
	R (Å)	ΔR (Å)	σ^2 (Å ⁻²)	R (Å)	ΔR (Å)	σ^2 (Å ⁻²)	R (Å)	ΔR (Å)	σ^2 (Å ⁻²)	R (Å)	ΔR (Å)	σ^2 (Å ⁻²)
ELETTRA	2.55	-0.004 ± 0.003	0.0078 ± 0.0007	3.59	-0.012 ± 0.013	0.0112 ± 0.0019	4.46	0.037 ± 0.008	0.0095 ± 0.0012	5.14	0.039 ± 0.008	0.0109 ± 0.0014
BNL	2.54	-0.006 ± 0.004	0.0073 ± 0.0009	3.58	-0.028 ± 0.015	0.0108 ± 0.0023	4.45	0.032 ± 0.009	0.0089 ± 0.0013	5.14	0.032 ± 0.008	0.0106 ± 0.0015
SSRL	2.55	-0.001 ± 0.006	0.0073 ± 0.0013	3.63	0.019 ± 0.011	0.0115 ± 0.0034	4.45	0.040 ± 0.013	0.0086 ± 0.0019	5.14	0.040 ± 0.011	0.0102 ± 0.0021
RRCAT	2.52	-0.032 ± 0.009	0.0081 ± 0.0026	3.54	-0.067 ± 0.021	0.0071 ± 0.0028	4.41	-0.008 ± 0.028	0.0096 ± 0.0040	5.17	0.066 ± 0.028	0.0116 ± 0.0026

Abbreviations and symbols used are explained in text.

Comparative study of EXAFS beamlines

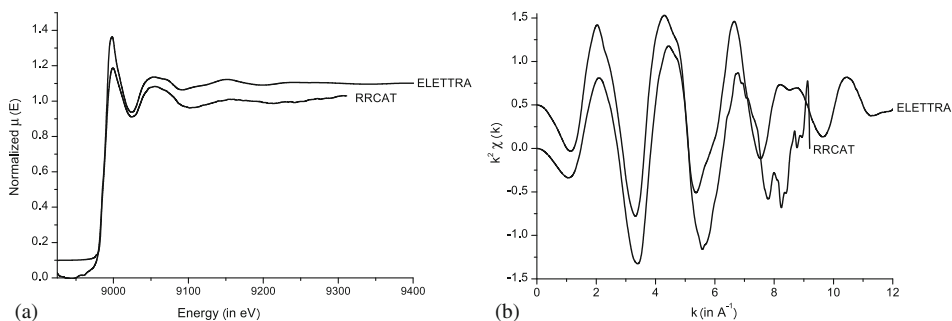


Figure 3. (a) Normalized Cu metal K-edge EXAFS spectra for copper complex obtained from two different synchrotron EXAFS beamlines. (b) k^2 -weighted $\chi(k)$ spectra obtained from normalized $\mu(E)$ spectra given in (a).

of goodness-of-fit parameter χ^2_v are 95.42, 172.19, 111.22 and 98.43 ELETTRA, BNL, SSRL and RRCAT data, respectively.

Thus, it can be seen that the local structure parameters obtained from the data recorded at the BL-8 beamline are sufficiently comparable to those obtained from the data recorded at the three other beamlines. However, as seen in table 2, the error bars for RRCAT values have been observed to be higher compared to the values from other synchrotron facilities. This may be due to the polychromator used on this beamline. Another reason may be the size of the pixels in the CCD detector used, which is 13.5 micron and also the distance of the CCD detector from the sample. Yet another reason is the size of the focal spot of the synchrotron beam.

The present analysis of the copper metal K-edge EXAFS has thus amply shown that reliable EXAFS data can be obtained from BL-8 dispersive EXAFS beamline at RRCAT.

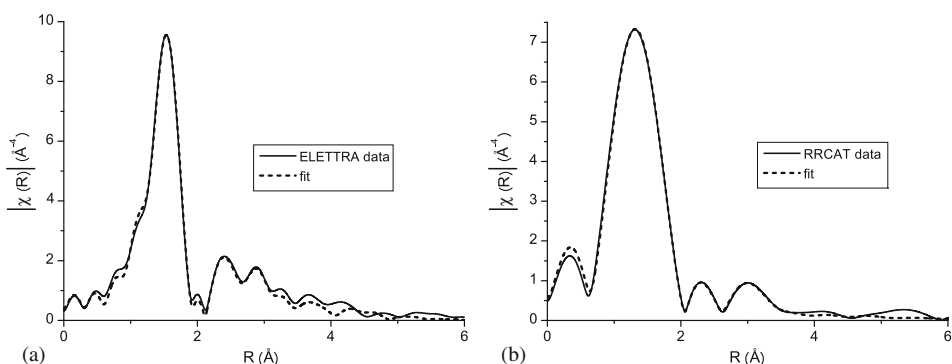


Figure 4. Magnitude of the Fourier transform of experimental data (solid line) along with theoretically modelled fit (dashed line). (a) ELETTRA and (b) RRCAT data. The data have been fitted using k weight of 3. The fitting parameters are given in the text.

Table 3. EXAFS fitting results for the copper complex. XRD results for the complex (from Bhadbhade *et al* [10]) are also given.

Atomic pair	Copper complex													
	EXAFS results (ELETTRA)					XRD results					EXAFS results (RRCAT)			
	N	R (Å)	ΔR (Å)	σ^2 (Å ⁻²)	R	N	R (Å)	ΔR (Å)	σ^2 (Å ⁻²)	R	N	R (Å)	ΔR (Å)	σ^2 (Å ⁻²)
Cu1-O2	1	1.86	-0.044 ± 0.009	0.0059 ± 0.0011	1.90	1	1.96	0.057 ± 0.096	0.0115 ± 0.0048					
Cu1-O1	1	1.90	-0.04 ± 0.002	0.0059 ± 0.0011	1.94	1	1.99	0.057 ± 0.096	0.0115 ± 0.0048					
Cu1-N1	1	1.95	-0.002 ± 0.005	0.0015 ± 0.0003	1.95	1	1.84	-0.115 ± 0.009	0.0096 ± 0.0051					
Cu1-N2	1	1.95	-0.002 ± 0.005	0.0015 ± 0.0003	1.95	1	1.84	-0.115 ± 0.009	0.0096 ± 0.0051					
Cu1-Oap	1	2.37	-0.044 ± 0.009	0.0055 ± 0.0011	2.41	1	2.47	0.057 ± 0.096	0.0115 ± 0.0048					

Abbreviations and symbols used are explained in text.

4.2 Copper complex

Figure 3a shows the Cu K-absorption edge of copper complex and the associated fine structure, obtained at the two different beamlines, viz., beamline 11.1 at ELETTRA and beamline BL-8 at RRCAT. Figure 3b shows their respective $\chi(k)$ vs. k plots. In both figures, the spectra have been shifted vertically by suitable values so that the spectra obtained by the two different beamlines may be easily compared with each other.

For the analysis of the ELETTRA data, the input parameter R_{bkg} was set to 1. Fourier transform was performed over k -range: $k_{\text{min}} = 2.73 \text{ \AA}^{-1}$ and $k_{\text{max}} = 12.93 \text{ \AA}^{-1}$. Theoretically modelled data were fitted in the R -space to the experimental data using $k_w = 3$ as shown in figure 4a. Fitting was performed in the R range of 1.0–4.0 \AA . In the fitting procedure, we have used the first 10 paths obtained after FEFF calculation. The value of goodness-of-fit parameter, i.e., reduced chi-square (χ_v^2) is 160. The results obtained from fitting are given in table 3, which gives the local structure parameters obtained from the analysis. The S_0^2 value so obtained is 0.93 with an error of ± 0.05 . ΔE_0 value is also reasonable, i.e., 1.81 eV with an error of ± 0.62 . The different ΔR values and σ^2 values determined are also listed in table 3.

For the analysis of the RRCAT data, the input parameter R_{bkg} was set to 1. Fourier transform was performed over k -range: $k_{\text{min}} = 2.789 \text{ \AA}^{-1}$, $k_{\text{max}} = 7.536 \text{ \AA}^{-1}$. Theoretically modelled data were fitted in the R -space to the experimental data using $k_w = 3$ as shown in figure 4b. Fitting was performed in the R ranges of 1–4 \AA . In the fitting procedure, we have used the first 10 paths obtained after FEFF calculation. The value of goodness-of-fit parameter, i.e., reduced chi-square (χ_v^2) is 19. The results obtained from fitting are given in table 3, which gives the local structure parameters obtained from the analysis. The S_0^2 value so obtained is 0.85 with an error of ± 0.15 . ΔE_0 value is also reasonable, i.e., 5.21 eV, with an error of ± 1.65 . The different ΔR values and σ^2 values determined are also listed in table 3.

The local structure parameters obtained from the RRCAT data are sufficiently comparable to those obtained from ELETTRA data. Also, these results are comparable with the crystallographic results reported by Bhadbhade *et al* [18] (table 3). Thus, even in weak EXAFS oscillation of a copper complex, we have found that the RRCAT data can be satisfactorily used for determining the local structure parameters.

5. Conclusions

The present work is a comparative study of the XAFS spectra recorded at the BL-8 beamline with those recorded at three other well-known synchrotron EXAFS beamlines. For this study, two examples have been taken, one of copper metal (the case of strong EXAFS oscillations) and the other of copper complex (the case of weak EXAFS oscillations). Theoretical models have been generated for both copper metal and the complex and fitted to their respective experimental EXAFS spectra to obtain the structural parameters. The structural parameters obtained by using BL-8 beamline have been found to be comparable to those obtained from other beamlines. Also, the results obtained from EXAFS data for the copper complex have been found to be comparable with the crystallographic results. Thus, it is seen that the spectra recorded at the BL-8 beamline can be satisfactorily used to

obtain the structural information around the absorbing atom of the sample. The quality of the recorded data has been found to be satisfactory because the noise is less and the beam is stable during the short period of recording of the data. The data have been found to be reliable because it is reproducible. However, it is advised that while using this beamline, a large number of spectra should be recorded for a sample and then data should be summed up. Further, the resolution of the beamline may be improved and the error bars in the fitting results may be reduced by the following measures:

- (i) By reducing the radius of curvature of the polychromator, i.e., by increasing the energy band.
- (ii) By reducing the size of the pixels in the CCD detector and also by increasing the distance of the CCD detector from the sample.
- (iii) By reducing the size of the focal spot of the synchrotron beam.

These measures are being considered for improving the performance of the beamline in future.

The present work is important in the Indian context because the beamline can be used by physicists, chemists and even biologists for determining molecular structure, especially the environment around the absorbing atom. The beamline is easily accessible to Indian users, which otherwise was not possible till now.

Acknowledgements

The authors thank Madhya Pradesh Council of Science & Technology (MPCST), Bhopal (India) for a research grant. XAFS measurements at ELETTRA were supported by an ICTP grant under the ICTP-ELETTRA Users Programme (proposal # 20105038). The support of BNL and SSRL staff for allowing one of the authors (BDS) to record the data is greatly acknowledged.

References

- [1] E A Stern, *J. Synchr. Rad.* **8**, 49 (2001)
- [2] F W Lytle, *J. Synchr. Rad.* **6**, 123 (1999)
- [3] G Bunker, *Introduction to XAFS – A practical guide to X-ray absorption fine structure spectroscopy* (Cambridge University Press, New York, 2010)
- [4] N C Das, S N Jha, D Bhattacharyya, A K Poswal, A K Sinha and V K Mishra, *Sadhana* **29**, 545 (2004)
- [5] D Bhattacharyya, A K Poswal, S N Jha, Sangeeta and S C Sabharwal, *Bull. Mater. Sci.* **32**, 103 (2009)
- [6] D Bhattacharyya, A K Poswal, S N Jha, Sangeeta and S C Sabharwal, *Nucl. Instrum. Methods* **A609**, 286 (2009)
- [7] A Gaur, A Johari, B D Shrivastava, D C Gaur, S N Jha, D Bhattacharyya, A Poswal and S K Deb, *Sadhana* **36**, 339 (2011)
- [8] A Gaur, B D Shrivastava, D C Gaur, J Prasad, K Srivastava, S N Jha, D Bhattacharyya, A Poswal and S K Deb, *J. Coord. Chem.* **64**, 1265 (2011)
- [9] S D Kelly, D Hesterberg and B Ravel, *Methods of soil analysis, Part 5, Mineralogical methods*, Chapter 14 (Soil Science Society of America, Medison, 2008)

Comparative study of EXAFS beamlines

- [10] C Y Yang and J E Penner-Hahn, *NSLS X – 19 A beamline performance for X-ray absorption measurements* (SRI-89 Conference, Berkeley, CA, 1989)
- [11] A Di Cicco, G Aquilanti, M Minicucci, E Principi, N Novello, A Cognigni and L Olivi, *J. Phys.: Conf. Ser.* **190**, 012043 (2009)
- [12] G Aquilanti *et al.*, *Dalton Trans.* **40**, 2764 (2011)
- [13] B Ravel and M Newville, *J. Synchr. Rad.* **12**, 537 (2005)
- [14] M Newville, B Ravel, D Haskel and E A Stern, *Physica* **B208** and **209**, 154 (1995)
- [15] S I Zabinsky, J J Rehr, A Ankudinov, R C Albers and M J Eller, *Phys. Rev.* **B52**, 2995 (1995)
- [16] M Newville, P Livins, Y Yacoby, J J Rehr and E A Stern, *Phys. Rev.* **B47**, 14126 (1993)
- [17] J J Rehr and R C Albers, *Rev. Mod. Phys.* **72**, 621 (2000)
- [18] M M Bhadbhade and D Srinivas, *Inorg. Chem.* **32**, 5458 (1993)
- [19] S D Kelly, S R Bare, N Greenlay, G Azevedo, M Balasubramaniam, D Barton, S Chattopadhyay, S Fakra, B Johannessen, M Newville, J Pena, G S Pokrovski, O Proux, K Priolkar, B Ravel and S M Webb, *J. Phys. Conf. Ser.* **190**, 012032 (2009)